International Journal of Applied Engineering Research ISSN 0973-4562 Volume 15, Number 4 (2020) pp. 385-392

Thermal Instability and Heat Transport in a Micropolar Fluid in the presence of Suction-Injection-Combination and Internal Heat Generation

Vasudha Yekasi[1], S Pranesh[2] and Shahnaz Bathul[1]

[1]*Department of Mathematics, Jawaharlal Nehru Technological University, Hyderabad, India.*

[2]*Department of Mathematics, Christ (Deemed to be University), Bangalore, India.*

Abstract

The effect of vertical throughflow or suction–injection–combination (SIC) on the thermal instability and heat transport in a micropolar fluid layer in the presence of internal heat generation, between permeable horizontal boundaries, when heated uniformly from below, is examined analytically. Using normal mode analysis, the eigenvalue is obtained for free–free velocity and isothermal temperature boundary condition on the spin-vanishing boundaries. Heat transport in the system is studied using Ginzburg Landau equation derived from Lorenz equations. The influence of various micropolar fluid parameters, Peclet number and internal Rayleigh number has been analysed by plotting the graphs.

Keywords: Micropolar Fluid, Rayleigh–Bénard convection, Suction–injection–combination, Internal heat generation.

1. INTRODUCTION

It is obvious that many of the industrially and technologically important fluids behave like a non-Newtonian fluid. Eringen [1,2] firstly formulated the theory of micropolar fluids and derived the constitutive laws for the fluids with microstructure. This theory provided a mathematical model for the non-Newtonian behaviour which could be observed in certain liquids such as polymers, colloidal suspensions, animal blood, liquids crystals etc. More interesting aspects of the theory and application of micropolar fluids can be found in the books of Eringen [3] and Lukazewicz [4] and in some studies of Peddieson and McNitt [5] , Willson [6], Siddheshwar and Pranesh [7]- [10], Pranesh and Riya Baby [11], Pranesh and et al [12-13].

Bénard [14] observed experimentally the origin of the classical Rayleigh problem of onset of convective instabilities in a horizontal layer of fluid which is heated from below there. Flow across the horizontal boundaries is not present in the standard classical problem. The modified problem where the boundaries are permeable and there is injection of liquid through the upper (or lower) plate and suction through the lower (or upper) plate called the throughflow or suction–injection–combination has been studied extensively by many authors (see [15]-[22]).

Thermal convection in horizontal fluid layer subject to constant but different temperatures at the boundaries have been extensively investigated by many researchers because of its importance in number of engineering and geophysical problems and in energy storage applications. In these problems control of convective instability plays an important role. One of the effective mechanisms to control the convective instability is maintaining a non-uniform temperature gradient across the fluid layer. The nonlinear temperature distribution in a horizontal fluid layer arising due to internal heat generation has been studied theoretically by Roberts [23], Takashima [24], Bhadauria et al. [25], Vasudha and Pranesh [26 – 28] , Pranesh et al [29-30].

In the paper, we study the effect of throughflow or suction–injection–combination on thermal instability and heat transport in a micropolar fluid layer in the presence of internal heat generation for free–free velocity and isothermal temperature boundary condition on the spin-vanishing boundaries.

2. MATHEMATICAL FORMULATION

An infinite horizontal layer of a Boussinesquian micropolar fluid layer of depth d is considered with the presence of internal heat generation. A Cartesian coordinate system (x, y, z) with origin in the lower boundary and z-axis vertically upwards is considered. Let ΔT be the temperature difference between the upper and lower boundaries (see Fig. (1)). A constant flow in the vertical direction with magnitude w_0, known as SIC, is maintained at the boundaries.

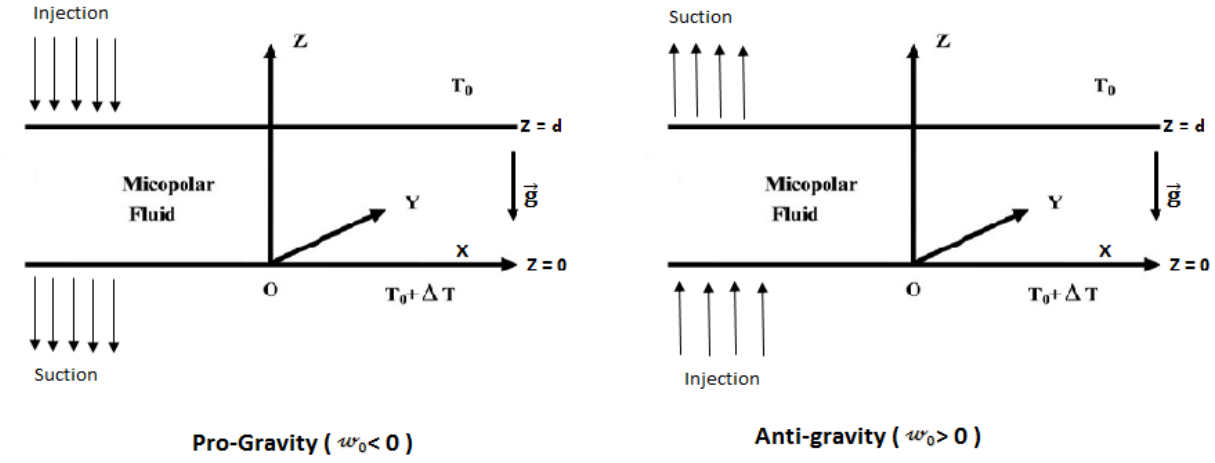

Figure 1: Schematic Diagram of the Flow Configuration

The governing equations which represent the above physical configuration are:

Continuity Equation:

$$\nabla.\vec{q} = 0 \ , \tag{1}$$

Conservation of Linear Momentum:

$$\rho_0\left[\frac{\partial\vec{q}}{\partial t} + (\vec{q}.\nabla)\vec{q}\right] = -\nabla p + \rho\vec{g}\hat{k} + (2\zeta+\eta)\nabla^2\vec{q} + \zeta(\nabla\times\vec{\omega}) \ , \tag{2}$$

Conservation of Angular Momentum:

$$\rho_0 I\left[\frac{\partial\vec{\omega}}{\partial t} + (\vec{q}.\nabla)\vec{\omega}\right] = (\lambda'+\eta')\nabla(\nabla.\vec{\omega}) + \eta'\nabla^2\vec{\omega} + \zeta(\nabla\times\vec{q} - 2\vec{\omega}), \tag{3}$$

Conservation of Energy:

$$\frac{\partial T}{\partial t} + (\vec{q}.\nabla)T = \frac{\beta}{\rho_0 C_v}(\nabla\times\vec{\omega}).\nabla T + \chi\nabla^2 T + Q(T-T_0) \ , \tag{4}$$

Equation of State:

$$\rho = \rho_0[1-\alpha(T-T_0)], \tag{5}$$

where, $\vec{q}$ is the velocity, ρ_0 is density of the fluid at temperature T = T_0, p is the pressure, ρ is the density, $\vec{g}$ is acceleration due to gravity, ζ is coupling viscosity coefficient or vortex viscosity, $\vec{\omega}$ is the angular velocity, I is moment of inertia, λ' and η' are bulk and shear spin viscosity coefficients, T is the temperature, χ is the thermal conductivity, β is micropolar heat conduction coefficient, α is coefficient of thermal expansion, η is the shear spin-viscosity coefficient, C_v is the specific heat, Q is the internal heat source and t is time.

3. BASIC STATE

The basic state is assumed to be quiescent and the quantities in the state are given by:

$$\vec{q} = w_0\hat{k},\ \vec{\omega} = \overrightarrow{\omega_b}(0,0,0),\ p = p_b(z),\ \rho = \rho_b(z),\ T = T_b(z)\ . \tag{6}$$

Substituting equation (6) into equations (1) – (5), we get the following basic state equations,

$$\frac{dp_b}{dz} = -\rho_b g, \tag{7}$$

$$w_0\frac{dT_b}{dz} = \chi\frac{d^2T_b}{dz^2} + Q(T_b - T_0)\ , \tag{8}$$

$$\rho_b = \rho_0[1-\alpha(T_b-T_0)]\ , \tag{9}$$

where, b refers the basic state, w_0 is the strength of the imposed constant suction (or injection) and $\hat{k}$ is the unit vector in the z-direction.

Solving equation (9) for T_b subject to the following boundary conditions

$T_b = T_0 + \Delta T$ *at* $z = 0$ *and* $T_b = T_0$ *at* $z = d$, we get

$$T_b(z) = \frac{\Delta T}{e^{m_1 d} - e^{m_2 d}}[e^{m_1 d}e^{m_2 z} - e^{m_2 d}e^{m_1 z}] + T_0 \tag{10}$$

where

$$m_1 = \frac{1}{2}\left[\frac{w_0}{\chi} + \sqrt{\frac{w_0^2}{\chi^2} - 4*\frac{Q}{\chi}}\right],\ m_2 = \frac{1}{2}\left[\frac{w_0}{\chi} - \sqrt{\frac{w_0^2}{\chi^2} - 4*\frac{Q}{\chi}}\right]. \tag{11}$$

4. LINEAR STABILITY ANALYSIS

The finite amplitude perturbations on the basic state are superposed in the following form:

$$\vec{q} = w_0\hat{k} + \overrightarrow{q'},\ \vec{\omega} = \overrightarrow{\omega_b} + \overrightarrow{\omega'}, p = p_b + p', T = T_b + T', \rho = \rho_b + \rho', \tag{12}$$

where the prime indicates that the quantities are infinitesimal perturbations.

Substituting equation (12) into the equations (1)-(5) and using the basic state solutions, we get linearized equations governing the infinitesimal perturbations in the form:

$$\nabla.\overrightarrow{q'} = 0\,, \tag{13}$$

$$\rho_0\left[\frac{\partial\overrightarrow{q'}}{\partial t} + (\overrightarrow{q'}.\nabla)\overrightarrow{q'} + w_0\frac{\partial\overrightarrow{q'}}{\partial z}\right] = -\nabla p' - \rho' g\hat{k} + (2\zeta+\eta)\nabla^2\overrightarrow{q'} + \zeta(\nabla\times\overrightarrow{\omega'})\,, \tag{14}$$

$$\rho_0 I\left[\frac{\partial\overrightarrow{\omega'}}{\partial t} + (\overrightarrow{q'}.\nabla)\overrightarrow{\omega'} + w_0\frac{\partial\overrightarrow{\omega'}}{\partial z}\right] = (\lambda'+\eta')\nabla(\nabla.\overrightarrow{\omega'}) + \eta'\nabla^2\overrightarrow{\omega'} + \zeta(\nabla\times\overrightarrow{q'} - 2\overrightarrow{\omega'})\,, \tag{15}$$

$$\frac{\partial T'}{\partial t} + w_0\frac{\partial T'}{\partial z} = \frac{\partial T_b}{\partial z}\left[\frac{\beta}{\rho_0 C_\vartheta}\nabla\times\overrightarrow{\omega'} - W'\right] + \chi\nabla^2 T' + QT' \tag{16}$$

$$\rho' = -\alpha\rho_0 T'. \tag{17}$$

Substituting equation (17) in equation (14), differentiating x-component of the equation with respect to z, differentiating z-component of the equation with respect to x and subtracting the two resultant equations, we get

$$\rho_0\left[\frac{\partial}{\partial t}\left(\frac{\partial u'}{\partial z} - \frac{\partial w'}{\partial x}\right) + u'\left(\frac{\partial^2 u'}{\partial x\partial z} - \frac{\partial^2 w'}{\partial x^2}\right) + w'\left(\frac{\partial^2 u'}{\partial z^2} - \frac{\partial^2 w'}{\partial x\partial z}\right) + w_0\frac{\partial}{\partial z}\left(\frac{\partial u'}{\partial z} - \frac{\partial w'}{\partial x}\right)\right] = -\rho_0\alpha g\frac{\partial T'}{\partial x} + (2\zeta+\eta)\nabla^2\left(\frac{\partial u'}{\partial z} - \frac{\partial w'}{\partial x}\right) + \zeta\left(\frac{\partial^2\omega_y}{\partial y\partial z} - \frac{\partial^2\omega_y}{\partial z^2} - \frac{\partial^2\omega_y}{\partial x^2} - \frac{\partial^2\omega_y}{\partial x\partial y}\right) \quad . \tag{18}$$

Writing y-component of the equation (15) we get

$$\rho_0 I\left[\frac{\partial\omega_y}{\partial t} + w_0\frac{\partial\omega_y}{\partial z} + \left(u'\frac{\partial}{\partial x} + w'\frac{\partial}{\partial z}\right)\omega_y\right] = \eta'\nabla^2\omega_y + \zeta\left(\frac{\partial u'}{\partial z} - \frac{\partial w'}{\partial x} - 2\omega_y\right) \tag{19}$$

Introducing the stream functions in the form

$$u' = \frac{\partial\psi}{\partial z}, w' = -\frac{\partial\psi'}{\partial x}, \tag{20}$$

which satisfies the continuity equation (13).

On using equations (20) in equations (16), (18) and (19), we get

$$\rho_0\left[\frac{\partial}{\partial t}(\nabla^2\psi) + w_0\frac{\partial}{\partial z}(\nabla^2\psi)\right] = -\rho_0\alpha g\frac{\partial T'}{\partial x} + (2\zeta+\eta)\nabla^4\psi - \zeta\left(\nabla^2\omega_y\right) + \rho_0 J(\psi,\nabla^2\psi) \tag{21}$$

$$\rho_0 I\left[\frac{\partial\omega_y}{\partial t} + w_0\frac{\partial\omega_y}{\partial z}\right] = \eta'\nabla^2\omega_y + \zeta\left(\nabla^2\psi - 2\omega_y\right) + I\rho_0 J\left(\psi,\omega_y\right) \tag{22}$$

$$\frac{\partial T}{\partial t} + w_0\frac{\partial T}{\partial z} = \frac{\partial T_b}{\partial z}\left[\frac{\beta}{\rho_0 C_\vartheta}\frac{\partial\omega_y}{\partial x} + \frac{\partial\psi}{\partial x}\right] + \chi\nabla^2 T + QT + \frac{\beta}{\rho_0 C_\vartheta}J\left(\omega_y, T\right) + J(\psi,T) \tag{23}$$

where, J stands for Jacobian.

Let $(x^*, y^*, z^*) = \left(\frac{x}{d}, \frac{y}{d}, \frac{z}{d}\right)$, $\psi^* = \frac{\psi}{\frac{\chi}{d}}$,

$$T^* = \frac{T}{\Delta T}\,,\ t^* = \frac{t}{d^2/\chi}\ ,\quad \omega_y^* = \frac{\omega_y}{\chi/d^2}\,. \tag{24}$$

Using equation (24) into equations (21)-(23) we get the dimensionless equations in the form (on dropping the asterisks for simplicity)

$$\frac{1}{Pr}\frac{\partial}{\partial t}(\nabla^2\psi) + \frac{Pe}{Pr}\frac{\partial}{\partial z}(\nabla^2\psi) = -R\frac{\partial T}{\partial x} + (1+N_1)\nabla^4\psi - N_1\nabla^2\psi + \frac{1}{Pr}J(\psi,\nabla^2\psi)\ , \tag{25}$$

$$\frac{N_2}{Pr}\frac{\partial\omega_y}{\partial t} + N_2\frac{Pe}{Pr}\frac{\partial\omega_y}{\partial z} = N_3\nabla^2\omega_y + N_1\nabla^2\psi - 2N_1\omega_y + \frac{N_2}{Pr}J(\psi,\omega_y), \tag{26}$$

$$\frac{\partial T}{\partial t} + Pe\frac{\partial T}{\partial z} = \frac{\partial T_0}{\partial z}\left[W + N_5\omega_y\right] + \nabla^2 T + Ri\,T + N_5 J\left(\omega_y, T\right) + J(\psi,T)\,, \tag{27}$$

The dimensionless parameters are

$Pe = \frac{w_0 d}{\chi}$, (Peclet Number)

$Pr = \frac{\zeta+\eta}{\chi\rho_0}$, (Prandtl Number)

$R = \frac{\rho_0\alpha g_0\Delta T d^3}{\chi(\zeta+\eta)}$, (Rayleigh Number)

$N_1 = \frac{\zeta}{\zeta+\eta}$, (Coupling Parameter)

$N_2 = \frac{I}{d^2}$, (Inertia Parameter)

$N_3 = \frac{\lambda'+\eta'}{(\zeta+\eta)d^2}$, (Couple Stress Parameter)

$N_5 = \frac{\beta}{\rho_0 C_\vartheta d^2}$, (Micropolar Heat Conduction Parameter)

$Ri = \frac{Qd^2}{\chi}$. (Internal Rayleigh Number)

In equation (27), $\frac{\partial T_0}{\partial z}$ is the non-dimensional form of $\frac{\partial T_b}{\partial z}$, where

$$\frac{\partial T_0}{\partial z} = \frac{1}{e^{w_1} - e^{w_2}}\left[w_2 e^{w_1} e^{w_2 z} - w_1 e^{w_2} e^{w_1 z}\right], \tag{28}$$

where $w_1 = \frac{Pe+\sqrt{Pe^2-4Ri}}{2}$, $w_2 = \frac{Pe-\sqrt{Pe^2-4Ri}}{2}$ (29)

Equations (25)-(27) are solved for free-free, isothermal, permeable and no-spin boundaries and hence we have

$$\psi = \frac{\partial^2\psi}{\partial z^2} = T = \omega_y = 0 \ at\ z = 0, 1.$$

By considering marginal state**,** in this section, we discuss the linear stability analysis, which is of great utility in the local nonlinear stability analysis to be discussed further on. The linearized version of equations (25)-(27), after neglecting the Jacobian , is

$$\left[\frac{1}{Pr}\frac{\partial}{\partial t} + \frac{Pe}{Pr}\frac{\partial}{\partial z} - (1+N_1)\nabla^2\right]\nabla^2\psi = -R\frac{\partial T}{\partial x} - N_1\nabla^2\omega_y\,, \tag{30}$$

$$\left[\frac{N_2}{Pr}\frac{\partial}{\partial t} + N_2\frac{Pe}{Pr}\frac{\partial}{\partial z} - N_3\nabla^2 + 2N_1\right]\omega_y = N_1\nabla^2\psi\,, \quad (31)$$

$$\left[\frac{\partial}{\partial t} + Pe\frac{\partial}{\partial z} - \nabla^2 T - Ri\right]T = \frac{\partial T_0}{\partial z}\left[W + N_5\omega_y\right] \quad (32)$$

We assume the solution of equations (30)-(32) to be periodic waves of the form

$$\left.\begin{aligned}\psi &= \psi_0 Sin(\pi\alpha x)Sin(\pi z)\\ \omega_y &= \Omega_0\, Sin(\pi\alpha x)Sin(\pi z)\\ T &= T_0 Cos(\pi\alpha x)Sin(\pi z)\end{aligned}\right\} \quad (33)$$

Substituting equation (33) into equations (30)-(32), we get

$$\begin{bmatrix}(1+N_1)k^4 & N_1k^2 & R\pi\alpha\\ N_1k^2 & 2N_1+N_3k^2 & 0\\ \frac{\partial T_0}{\partial z}\pi\alpha & \frac{\partial T_0}{\partial z}N_5\pi\alpha & Ri-k^2\end{bmatrix}\begin{bmatrix}\psi_0\\ \Omega_0\\ T_0\end{bmatrix} = \begin{bmatrix}0\\0\\0\end{bmatrix} \quad (34)$$

where $k^2 = \pi^2(\alpha^2+1)$.

For a non-trivial solution of the homogeneous system (34) for $\psi_0, \Omega_0\ and\ T_0$, the determinant of the coefficient matrix must vanish. This leads on simplification to

$$R = \frac{N_3(1+N_1)k^8 + N_1(2+N_1)k^6 - Ri(N_3(1+N_1)k^6 + N_1(2+N_1)k^4)}{\pi^2\alpha^2 g(z)(N_3k^2 + 2N_1 - N_1N_5k^2)} \quad (35)$$

where g(z)=-$\int_0^1 \frac{\partial T_0}{\partial z}(Sin[\pi z])\text{^}2dz$.

5. FINITE AMPLITUDE CONVECTION

The finite amplitude analysis is carried out here via Fourier series representation of stream function ψ, the spin $\omega_y$and the temperature distribution T.As linear analysis is inadequate to explain the rate of heat transfer as it is sufficient for obtaining the stability condition for the onset of convection, the study of linear analysis is important to extract the information on rate of heat transfer.

The first effect of non-linearity is to distort the temperature field through the interaction of ψ and T. The distortion of temperature field will correspond to a change in the horizontal mean, i.e., a component of the form $Sin(2\pi z)$ will be generated. Thus a minimal double Fourier series which describes the finite amplitude convection is given by

$$\psi(x,y,t) = A(t)Sin(\pi\alpha x)Sin(\pi z) \quad (36)$$

$$\omega_y(x,y,t) = B(t)\, Sin(\pi\alpha x)Sin(\pi z) \quad (37)$$

$$T(x,y,t) = E(t)Cos(\pi\alpha x)Sin(\pi z) + F(t)Sin(\pi z) \quad (38)$$

where, A is the amplitude of the velocity convection, B is the amplitude of angular velocity convection, E and F are the amplitudes of the temperature to be determined from the dynamics of the system. Since the spontaneous generation of large scale flow has been discounted, the functions ψ and ω_y do not contain an x-independent term.

Substituting equations (36)-(38) into equations (25)-(27) and following standard orthogonalization procedure for the Galerkin expansion, we obtain the following non-linear autonomous system (generalized Lorenz model) of differential equations:

$$\dot{A} = \frac{-RPr\pi\alpha}{k^2}E - (1+N_1)Prk^2A - N_1PrB \quad (39)$$

$$\dot{B} = \frac{-N_3Prk^2}{N_2}B - \frac{N_1Prk^2}{N_2}A - \frac{2N_1Pr}{N_2}B \quad (40)$$

$$\dot{E} = \frac{\partial T_0}{\partial z}N_5\pi\alpha B + \frac{\partial T_0}{\partial z}\pi\alpha A - (k^2 - Ri)E - \pi^2\alpha N_5BF - \pi^2\alpha AF \quad (41)$$

$$\dot{F} = -4\pi^2F + RiF + \frac{\pi^2\alpha N_5}{2}BE + \frac{\pi^2\alpha}{2}AE \quad (42)$$

where over dot denotes time derivative with respect to *t*. It is important to observe that the non-linearities in equations (39)-(42) stem from the convective terms in the energy equation (4) as in the classical Lorenz system.

6. THE GINZBURG-LANDAU EQUATION FROM LORENZ MODEL

From equations (39)-(41) we have

$$A = -\frac{N_2}{N_1Prk^2}\dot{B} - \left[\frac{N_3}{N_1} + \frac{2}{k^2}\right] \quad B = -Y_1\dot{B} - Y_2B, \quad (43)$$

$$E = -\frac{k^2}{RPr\pi\alpha}\dot{A} - \frac{(1+N_1)k^4}{R\pi\alpha}A - \frac{N_1k^2}{R\pi\alpha}B, \quad (44)$$

$$F = \frac{1}{N_5\pi^2\alpha B + \pi^2\alpha A}\left[-\dot{C} + \frac{\partial T_0}{\partial z}\pi\alpha N_5B + \frac{\partial T_0}{\partial z}\pi\alpha A - (k^2 - Ri)E\right] \quad (45)$$

Using equation (43) in equation (44) and then using the resulting equation along with equation (43) in (45), we get

$$E = Y_3\ddot{B} + Y_4\dot{B} + Y_5B\ , \quad (46)$$

$$F = \frac{1}{Y_6\dot{B} + Y_7B}\left[-Y_3\dddot{B} + Y_8\ddot{B} + Y_9\dot{B} + Y_{10}B\right], \quad (47)$$

where

$$Y_1 = \frac{N_2}{N_1Prk^2}, \quad Y_2 = \frac{N_3}{N_1} + \frac{2}{k^2},$$

$$Y_3 = \frac{Y_1k^2}{RPr\pi\alpha}, \quad Y_4 = \frac{Y_2 + (1+N_1)Prk^2Y_1}{RPr\pi\alpha},$$

$$Y_5 = \frac{[(1+N_1)Prk^2Y_2 - N_1Pr]k^2}{RPr\pi\alpha}, \quad Y_6 = -\pi^2\alpha Y_1\,,$$

$$Y_7 = \pi^2\alpha N_5 - \pi^2\alpha Y_2\,, \quad Y_8 = -Y_4 - k^2 + Ri$$

$$Y_9 = -Y_5 - \frac{\partial T_0}{\partial z}\pi\alpha Y_1 - k^2Y_4 + RiY_4\,,$$

$$Y_{10} = -\frac{\partial T_0}{\partial z}\pi\alpha Y_2 + \frac{\partial T_0}{\partial z}\pi\alpha N_5 - k^2Y_5 + RiY_5$$

Substituting equations (43), (46) and (47) in equation (42), we get a third order equation in B after neglecting the terms of the type

$\frac{\partial^4 B}{\partial t^4}, \frac{\partial^3 B}{\partial t^3}, \frac{\partial^2 B}{\partial t^2}, B\left(\frac{\partial B}{\partial t}\right)^2, \left(\frac{\partial B}{\partial t}\right)^2, B^2\frac{\partial B}{\partial t}, B\frac{\partial^3 B}{\partial t^3}, B\frac{\partial^2 B}{\partial t^2}$.

$$P_1\frac{\partial B}{\partial t} = P_2B - P_3B^3 \quad (48)$$

where

$$P_1 = (4\pi^2 - Ri)[Y_9Y_7 + Y_{10}Y_6]\,,$$

$$P_2 = (-4\pi^2 + Ri)Y_{10}Y_7\,,$$

$P_3 = \left[\frac{\pi^2\alpha}{2} Y_2 Y_5 Y_7^2 - \frac{\pi^2\alpha N_5}{2} Y_5 Y_7^2\right]$.

Equation (48) is obviously the Ginzburg-Landau model for non-linear convection in a micropolar fluid with suction injection combination and heat source.

Substituting Equation (48) in equation (47), we get *F* in terms of *B*.

7. HEAT TRANSPORT

The influence of Suction Injection combination with internal heat source on heat transport which is quantified in terms of Nusselt number (Nu) is defined as follows:

$$Nu = \frac{Heat\ transport\ by\ (conduction+convection)}{Heat\ transport\ by\ (conduction)}$$

$$= \frac{\left[\frac{k_c}{2\pi}\int_0^{2\pi/k_c}(1-z+T)_z dx\right]_{z=0}}{\left[\frac{k_c}{2\pi}\int_0^{2\pi/k_c}(1-z)_z dx\right]_{z=0}} . \quad (49)$$

where subscript in the integrand denotes the derivative with respect to z.

Substituting equation equation (38) in equation (49) and completing the integration, we get

$$Nu = 1 - 2\pi F(t) .$$

8. RESULTS AND DISCUSSIONS

As made out in the introduction of the paper, there are numerous papers considering the individual effects of

i) suction-injection combination,

ii) micropolar fluid and

iii) internal heat generation.

In the present paper, a linear and non-linear study is made on the combination of the above effects on thermal instability and heat transport. These three effects are, respectively, represented by the Peclet number *Pe*, the micropolar heat conduction parameters and the internal Rayleigh number *Ri*.

In linear analysis, normal mode technique is applied to find the expression for Rayleigh number and wave number as a function of internal Rayleigh number, Peclet number, micropolar heat conduction parameter, Prandtl number, coupling parameter, couple stress parameter and inertia parameter. Figures (2) to (4) are plots of Rayleigh number *R* versus the Peclet number *Pe* for the onset of convection. Before embarking on a discussion of the results depicted by the figures (2) to (4), we note that the principle of exchange of stabilities (PES) is valid in the problem. The parameter *Ri* may take both negative and positive values. Positive values indicate internal heat generation and negative values indicate internal heat absorption. The negative value of parameter *Pe* represents pro-gravity and positive value of *Pe* represents anti-gravity. The thermodynamic restriction permits the values of $N_1, N_3, and\ N_5$ to lie in the following ranges (Siddheshwar and Pranesh [8]) :

$0 \le N_1 \le 1$, $0 \le N_2 \le r$, $0 \le N_3 \le m$, $0 \le N_5 \le n$,

where the quantities *r, m* and *n* are finite positive real numbers.

In all the plots, we observe that as *Ri* changes from negative to positive, *R* is decreasing. Therefore, the onset of convection is advanced by the increase in heat supply due to the increase of *Ri*. Thus, increasing internal Rayleigh number *Ri* results in the destabilization of the system.

Figure (2) is the plot of *R* versus *Pe* for different values of Coupling Parameter $N_1$for free-free velocity, isothermal temperature and no spin boundary combinations. In these plot, the Rayleigh number increases with increasing of N_1 for all values of *Ri* considered. N_1 indicates the concentration of microelements, and increasing of N_1 is to elevate the concentration of microelements in number. When this happened, a greater part of the energy of the system is consumed by these elements in developing gyrational velocities of the fluid and thus delays the onset of convection.

Figure (3) is the plot of *R* versus *Pe* for different values of Couple stress parameter N_3 in case of free-free velocity, isothermal temperature and no spin boundary combinations. It can be clearly seen that in the presence of internal heating, an increase of N_3 decrease the values of *R*. This is because increase in N_3 decreases the micropolar spin diffusion of the fluid and hence makes the system more unstable.

Figure (4) is the plot of R_c versus *Pe* for different values of Micropolar Heat Conduction Parameter N_5 in case of free-free velocity, isothermal temperature and no spin boundary combinations. It is observed that the increase in N_5 results in the increase in *R*. The increase in N_5 increases the heat induced into the fluid, thereby reducing the heat transferred from the bottom to the top, which delays the onset of convection.

We now discuss the results obtained for non-linear analysis. Using the minimal representation of Fourier series, the fourth order Lorenz model is derived, which is analytically intractable. An analytically tractable Ginzburg Landau equation is derived from Lorenz model by using elimination method. Using the analytical solution of Ginzburg-Landau equation for the amplitude *B(t)*, the expression for Nusselt number, which quantities the amount of heat transfer is obtained as a function of *F(t)*. The results obtained are plotted in the figures (5)-(9).

Figures (5) to (9) are plots of Nusselt number versus time t for different values of Coupling parameter N_1, Inertia parameter N_2, Couple stress parameter N_3, Micropolar heat conduction parameter N_5 and Prandtl number *Pr* together with internal Rayleigh number *Ri* for both pro-gravity and anti-gravity cases. From these figures, it can be observed that increase in N_1 and N_5 decreases heat transfer and increase in N_2, N_3 and *Pr* increases heat transfer in the

system. But when it comes to the effect of internal Rayleigh number *Ri*, in pro-gravity case, increase in *Ri* increases the heat transfer whereas in anti-gravity case, increase in *Ri* decreases the heat transfer.

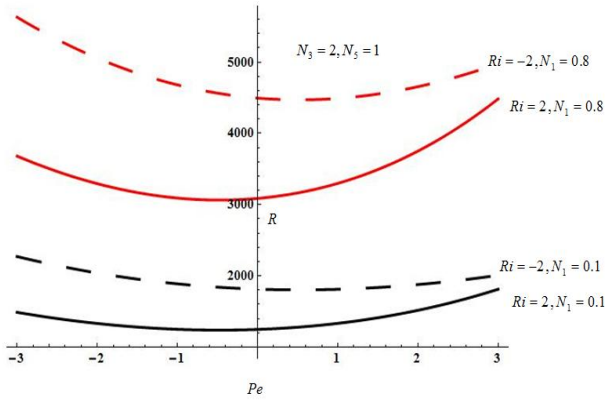

Figure 2: Plot of R versus Pe for different values of Coupling Parameter N_1 and internal Rayleigh number Ri.

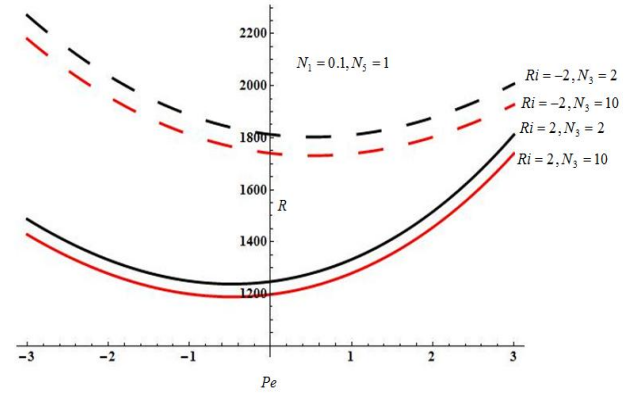

Figure 3: Plot of R versus Pe for different values of Couple stress Parameter N_3 and internal Rayleigh number Ri .

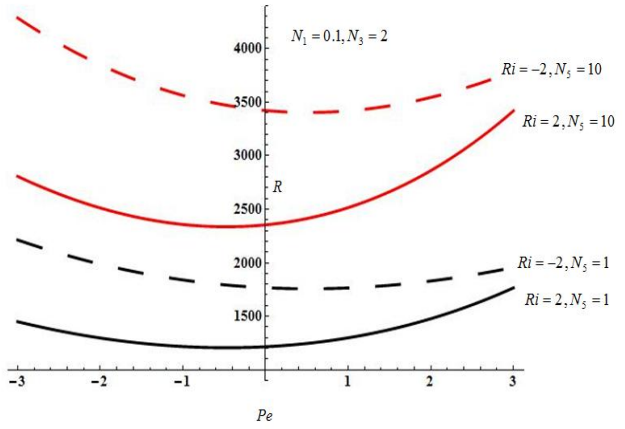

Figure 4: Plot of R versus Pe for different values of micropolar heat conduction parameter N_5 and internal Rayleigh number Ri .

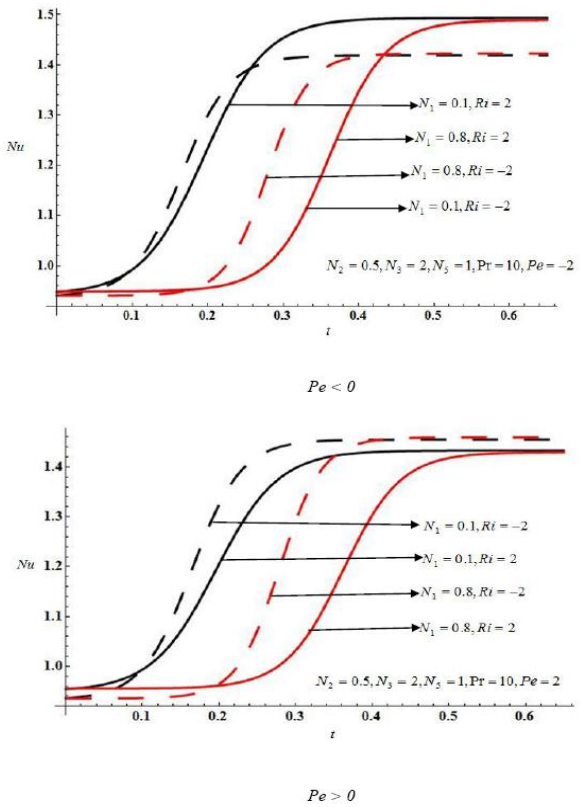

Figure 5: Plot of Nusselt Number Nu versus time t for different values of Coupling Parameter N_1 and internal Rayleigh number Ri for pro-gravity (Pe < 0) and anti-gravity (Pe > 0) cases.

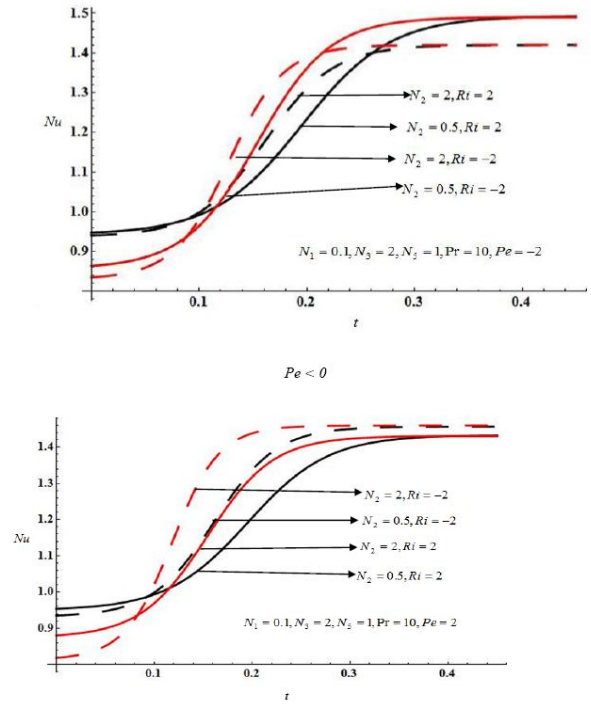

Figure 6: Plot of Nusselt Number Nu versus time t for different values of Inertia Parameter N_1 and internal Rayleigh number Ri for pro-gravity (Pe < 0) and anti-gravity (Pe > 0) cases.

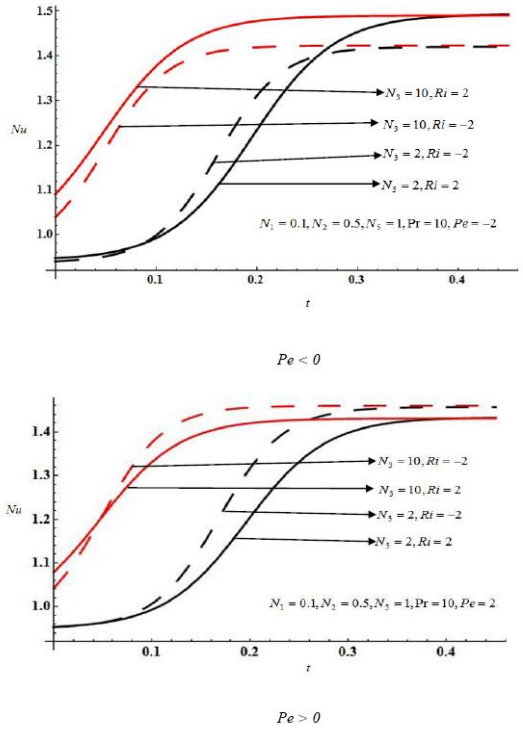

Figure 7: Plot of Nusselt Number Nu versus time t for different values of Couple stress Parameter N_3 and internal Rayleigh number Ri for pro-gravity (Pe < 0) and anti-gravity (Pe > 0) cases.

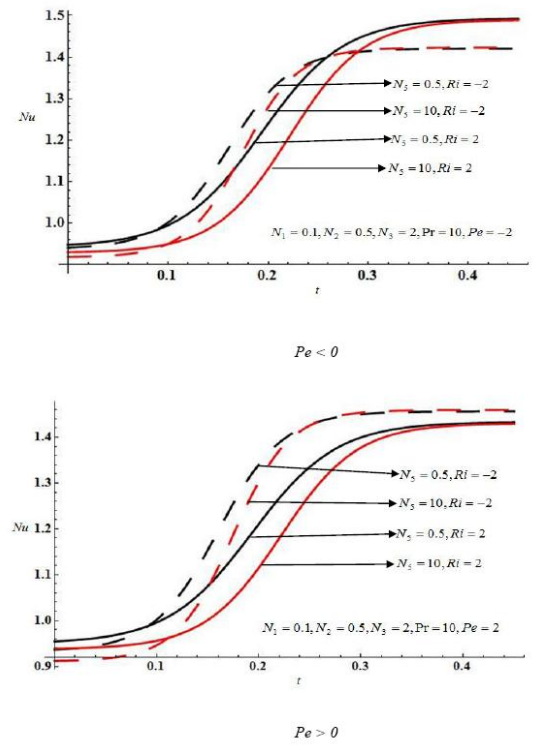

Figure 8: Plot of Nusselt Number Nu versus time t for different values of Micropolar Heat Conduction Parameter N_5 and internal Rayleigh number Ri for pro-gravity (Pe < 0) and anti-gravity (Pe > 0) cases.

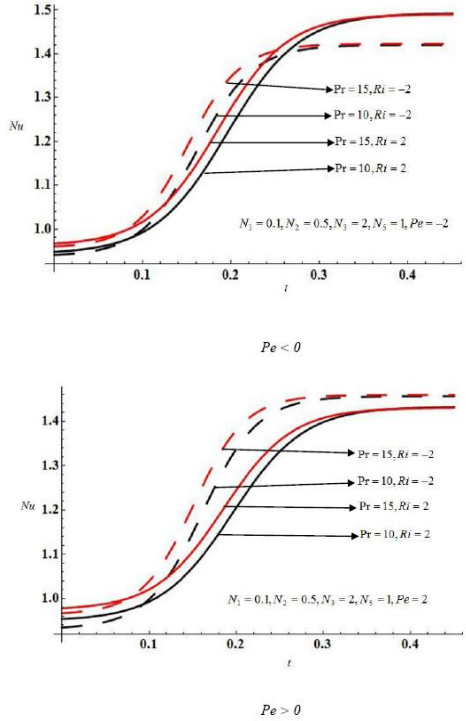

Figure 9: Plot of Nusselt Number Nu versus time t for different values of Prandtl Number Pr and internal Rayleigh number Ri for pro-gravity (Pe < 0) and anti-gravity (Pe > 0) cases.

9. CONCLUSIONS

Linear and non-linear stability analysis of suction-injection combination of the Rayleigh–Bénard convection in micropolar fluids with internal heat generation is investigated theoretically.

1. In pro-gravity case, increase in *Ri* enhances the heat transfer whereas in anti-gravity case, increase in *Ri* diminishes the heat transfer.
2. By adjusting the SIC it is possible to control the convection in micropolar fluids.
3. Rayleigh-Bénard convection in Newtonian fluids may be delayed by adding micron-sized suspended particles.

ACKNOWLEDGEMENT

The authors express their sincere gratitude to their respective institutions for encouragement and support.

REFERENCES

[1] A.C. Eringen, Theory of micropolar fluids, J. Math. Mech. 16 (1966) 1–18.

[2] A.C. Eringen, Theory of thermomicropolar fluids, J. Math. Anal. Appl. 38 (1972) 480–496.

[3] Eringen AC (2001) Microcontinuum field theories II: Fluent Media. Springer, Newyork.

[4] Lukaszewicz G (1999) Micropolar fluids: Theory and applications. Brikhauser Basel.

[5] Peddieson J, McNitt RP (1970) Boundary layer theory for micropolar fluid. Recent Adv Eng Sci 5: 405–426

[6] Willson AJ (1970) Boundary layers in micropolar liquids. Proc. Camb Phil Soc 67: 469–476

[7] Siddheshwar PG, Pranesh S (1998) Effect of a non-uniform basic temperature gradient on Rayleigh-Benard convection in a micropolar fluid. Int J Eng Sci 36: 1183–1196

[8] Siddheshwar PG, Pranesh S (2002) Magnetoconvection in fluids with suspended parti-cles under *lg* and *μg*. Aerospace Sci Tech 6: 105–114.

[9] Siddheshwar PG, Pranesh S (2005) Linear and weakly non-Linear analyses of convection in a micropolar fluid Hydrodynamics VI-Theory and Applications, 487-493.

[10] Siddheshwar PG, Pranesh S (2012) Effect of non-uniform basic concentration gradient on the onset of double-diffusive convection in micropolar fluid Applied mathematics 3 (05), 41.

[11] S. Pranesh, and Riya Baby, (2012), Effect of Non-Uniform Temperature Gradient on the Onset of Rayleigh-Bénard Electro Convection in a Micropolar Fluid, Applied Mathematics, Vol. 3, Pp. 442-450.

[12] TV Joseph, S Pranesh, S Manjunath (2017) Linear and Non-linear analysis of electrothermo convection in a micropolar fl uid J. Heat and Mass Transfer 14 (4), 461-484.

[13] A Mathew, M Jagannath, S Pranesh (2019) Inphase and outphase concentration modulation on the onset of magneto-convection and mass transfer in weak electrically conducting micropolar fluids AIP Conference Proceedings 2080 (1), 030012

[14] H. Bénard, (1901), Les Tourbillions Cellularies Dans une Nappe Liquide Transportant de la Chaleut par Convection en Regime Permanent, Annales de Chimie et de Physique, Vol. 23, Pp. 62.

[15] D. L. Shvartsblat, (1969), Steady Convection Motions in a Plane Horizontal Fluid Layer with Permeable Boundaries, Fluid Dynamics, Vol. 4, No. 5, Pp. 54-59.

[16] D. A. Nield, (1987), Through Flow Effects in the Rayleigh-Bénard Convective Instability Problem, Journal of Fluid Mechanics, Vol. 185, Pp. 353-360.

[17] P. G. Siddheshwar, and S. Pranesh, (2001), Suction-Injection Effects on the Onset of Rayleigh-Bénard-Marangoni Convection in a Fluid with Suspended Particles, Acta Mechanica, Vol. 152, Pp. 241-252.

[18] I. S. Shivakumara, and S. P. Suma, (2000), Effects of Through Flow and Internal Heat Generation on the Onset of Convection in a Fluid Layer, Acta Mechanica, Vol. 140, No. 3, Pp. 207-217.

[19] Y. N. Murty, and V. V. Ramana Rao, (2000), Effect of Through Flow on Marangoni Convection in Micropolar Fluids, Acta Mechanica, Vol. 138, No. 3, Pp. 211.

[20] Y. N. Murty, (2001), Effect of Through Flow and Magnetic Field on Bénard Convection in Micropolar Fluids, Acta Mechanica, Vol. 150, No. 1, Pp. 11-21.

[21] Y. N. Murty, (2006), Effect of Through Flow and Magnetic Field on Marangoni Convection in Micropolar Fluids, Applied Mathematics and Computation, Vol. 173, Pp. 1288-1299.

[22] S Pranesh (2018) Effect of Throughflow on the Onset of Electro-Thermo Convection in a Micropolar Fluid with Maxwell-Cattaneo Law Recent Trends in Fluid Mechanics 5 (1), 1-17

[23] Roberts P H 1967 Convection in horizontal layers with internal heat generation: Theory J. Fluid Mech. 30 33-49

[24] Takashima M," The stability of natural convection in an inclined fluid layer with internal heat generation", Journal of Physical Society of Japan, 58, 4431-4440, (1989).

[25] B. Bhadauria, A. Kumar, J. Kumar, N. Sacheti and P. Chandran,"Natural convection in a rotating anisotropic porous layer with internalheat generation", Transport in Porous Media, vol. 90, no. 2, pp.687-705, 2011.

[26] Vasudha Yekasi, S Pranesh and Shahnaz Bathul, (2016), "Effects of Gravity Modulation and Internal Heat Generation on the onset of Rayleigh-Bénard convection in a Micropolar Fluid", Journal of Advances in Mathematics, Vol. 12, pp 6270 - 6285 .

[27] Vasudha Yekasi, S Pranesh and Shahnaz Bathul, (2017), "Effects of Temperature Modulation and Internal Heat Generation on the onset of Rayleigh-Bénard convection in a Micropolar Fluid", Global Journal of Pure and Applied Mathematics, Vol. 13, pp. 2411-2437.

[28] Vasudha Yekasi, S Pranesh and Shahnaz Bathul, (2018), " Effect of internal heating on weakly non-linear stability analysis of Rayleigh-Bénard Convection in a vertically oscillating Micropolar fluid", International Journal of Applied Engineering Research, Vol. 13, pp. 11164-11171.

[29] HJ Priyanka, S Pranesh Effect of Internal Heat Generation on the Onset of Rayleigh-Bènard Chandrashekar Convection in a Micropolar Fluid with Maxwell Cattàneo Law Recent Trends in Fluid Mechanics 5 (1), 31-43.

[30] NS Arshika, MEH Oumar, S Pranesh Effect of Coriolis force on Rayleigh-Bénard convection with internal heat generation International Journal of Advanced Technology and Engineering Exploration 6 ,54, 133-142.